ANALYZING THE EFFECTS OF LAND USE / COVER CHANGE (LULCC) SIMULATION ON FLOODING: A CASE STUDY IN LAS NIEVES, AGUSAN DEL NORTE, MINDANAO, PHILIPPINES

M. Makinano-Santillan[1,2], K. P. Bolanio[1,2], J.D. Valeroso[2], L.G. Yu[2]

[1] Caraga Center for Geo-Informatics, Caraga State University, Butuan City, Philippines – mmsantillan@carsu.edu.ph
[2] Department of Geodetic Engineering, College of Engineering and Geosciences, Caraga State University, Butuan City, Philippines – (kpbolanio, jaymar.valeroso, lucille.yu)@carsu.edu.ph

Commission IV, WG7

Keywords: LULCC, Prediction, Flood Simulation, SVM, MOLUSCE, Sentinel-2

Abstract: The municipality of Las Nieves, located in Agusan del Norte, Mindanao, Philippines, has experienced floods and flood-related damages in the floodplain region in recent years. Despite the best intentions of planning and implementing projects anchored in its comprehensive land use plans, recurring flooding significantly impacts its residents. Due to its growing population, changes in land cover are inevitable. The changes can result in increased overland flow and decreased infiltration rates. This study was conducted to determine and quantify the effect of changing the land use/land cover (LULC) on the flooding condition in the municipality. Base LULC map was generated using Sentinel-2 image captured in 2021. Support Vector Machine classifier was used in the classification resulting in an accuracy of 94.07%. The 2021 LULC map was the reference for predicting future LULCs for 2025 and 2029 implemented in MOLUSCE and was utilized for flood simulation. HEC-HMS and HEC-RAS were used to generate flood depth maps of different extreme rainfall scenarios. The results showed that as the rainfall event increased, the extent of affected LULC areas also increased. Based on the rainfall impact assessment results, the annual cropland was the most impacted LULC class across the various LULC classes. The class open forest is the least affected class for 2021, 2025, and 2029. However, the barren was the least affected in the scenario-based build-up increase. These assessments are especially pertinent because storm-related rains have been increasingly severe recently and will continue due to climate change. The simulations and flood mapping knowledge can inform and empower the Local Government Unit of Las Nieves. It will guide them in developing informed decision frameworks for mitigating significant land surface variabilities and adapting effective future land use plans to reduce the adverse effects of flooding.

1. INTRODUCTION

A regular downpour typically brings about flooding throughout an extended timeframe or heavy rainfall throughout a brief period. Most flood studies rely on hydrological models such as rainfall-runoff models. They began as basic models and have progressed to complicated algorithms that can account for the unpredictability of water catchment conditions (Džubáková, 2010). However, research shows that human-related activities that cause land use/land cover changes, like deforestation and urbanization, can affect flooding (Brevante, 2017). Proper land use/land cover management can help prevent land degradation, mitigate climate change, and alleviate extreme rainfall events.

Although humans have been modifying land surfaces for thousands of years to gain a livelihood and other necessities, the intensity, area, and rate of land use/land cover change are considerably higher now than previously (Hassan et al., 2016). Remotely sensed data were used to track the dynamics of LULC change. These are available in various resolutions, e.g., spatial, spectral, and temporal, allowing for detecting changes on the earth's surface. Several studies in the previous decades have attempted to recognize and evaluate the impact of land development on floods (Reynard et al., 2001). While foregoing groundworks for this field of study are commonly directed in a retrospect manner, the conduct of this study must link patterns of different design storm structures with processes of future land use/land cover changes in Las Nieves. which includes two upstream watersheds that generate run-off to the concerned area and potentially cause flooding. Hence, the simulation and forecast of potential land use land cover change will be implemented, and the researchers will be able to examine its possible repercussions on the rainfall-runoff phenomena of the specified region. This direction can help determine the state of its LULCC in the following years and its probable environmental connotations, especially on flooding. Suppose the researchers will be able to perform an analysis of the effects of LULCC simulation on flooding. In that case, stakeholders can understand and provide input on minimizing human environmental impacts.

Despite the good intention of comprehensive land use plans, the change in LULC is a potential factor in increased overland flow and reduced infiltration capacity. Hence, it can induce faster peak time but slower peak discharge. Specifically for domains with significant built-up areas, indicating immediate but prolonged flooding for that particular catchment (de Moel & Aerts, 2011). By simulating future LULCC about an existing LULC base map and analyzing its effects as an integral part of the hydrological process in Las Nieves, the researchers will be able to evaluate better the role and relationship of subsequently predicted LULCC. And how will it affect the overland flow (rainfall-runoff) over time, e.g., if built-up areas will expand in the future, how will it impact flood scenarios, and to what extent? Thus, this research can provide helpful insights for the concerned local government units (LGU) to develop informed decision frameworks for mitigating significant land surface variabilities and adapting effective future land use plans in the specified study area.

The accuracy of the LULCC simulation and its corresponding effect on the rainfall-runoff phenomena with varying rainfall scenarios will be determined and sustained by available source datasets as well as the software and algorithms to be utilized and, consequently, the modeling and assessment methods to be followed and applied. Since the hydrological process of rainfall-runoff simulation will be inherently dependent on the existing LULC condition of the chosen area, the implications of LULCC rainfall-runoff dynamics to be analyzed will concentrate on the

study area only, as shown in Figure 1. These desired insights will not be necessarily applicable and practical to other nearby regions.

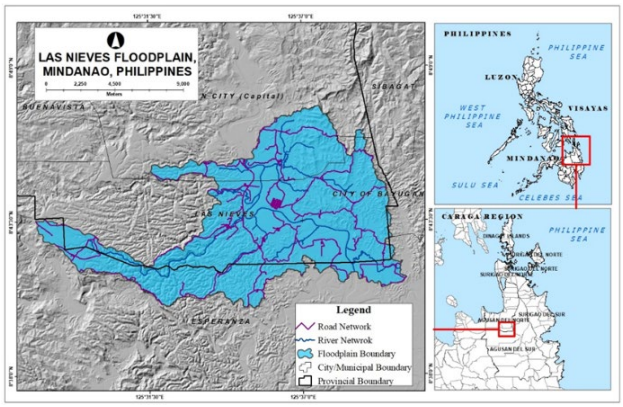

Figure 1. Las Nieves floodplain area, Agusan del Norte, Mindanao, Philippines.

2. METHODOLOGY

In generating the base LULC for LULCC simulation, integrated multispectral satellite imageries including of the present scene of the study area were subjected to pre-processing techniques. Support Vector Machine (SVM) was utilized to generate the LULC base map. The researchers proposed crucial changes to the land cover from the generated base LULC map and then tested the new LULC map for flood simulation purposes. A series of LULC maps were used for flood simulation using flood models of the upstream watersheds in reference to the study area to simulate hypothetical rainfall scenarios with different return periods (2YR, 5YR,10YR, 25YR, 50YR,100YR) that were implemented through HEC-RAS. An assessment of the predicted LULCC's impact on rainfall-runoff in Las Nieves floodplain to determine how it would influence extreme rainfall events in the future was then conducted. The entire methodology used to answer the objectives is shown in Figure 2.

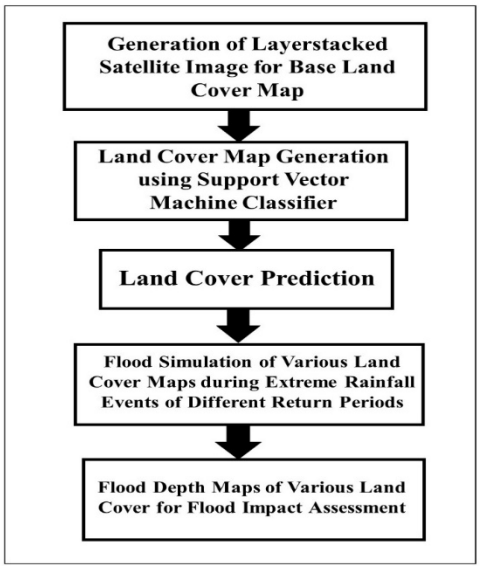

Figure 2. Methodological flow diagram

2.1. Land cover generation

The land cover mapping for the base LULC generation employed a supervised Support Vector Machine (SVM) classifier implemented in ArcGIS software using Sentinel-2 L2 image dated July 2021. The SVM is a supervised classification algorithm that works similarly to the Maximum Likelihood Classification (MLC) classifiers. It looks at multidimensional positions formed by each training sample's band attributes or values. Instead of calculating the probability that a pixel is adherent to a class cluster, the SVM method specifies the multidimensional environment so that the separation among the class clusters is as wide as attainable. For the selection of validation points, at least 50 points per land cover class were considered for assessing the accuracy of the base land use/land cover map of Las Nieves. Google Earth's high-resolution satellite images are to be used to verify these random points by overlaying the validation points from the established land cover map on top of the available images of the latter software (Santillan et al., 2016). Land cover classes present in the area are: Annual Cropland, Built-up, Open Forest, Shrubs, Barren, Grassland, Perennial Cropland, and Water.

2.2. Land cover prediction

Prediction of LULC was employed in MOLUSCE (Module for Land Use Change Simulation), a user-friendly QGIS 2.0 and above plugin for analyzing, modeling, and simulating LULC changes (Alam et al., 2021). Two land cover inputs (2015 and 2017) were fed into the plugin to simulate the land cover for 2021 and validate it using the generated 2021 land cover. The spatial variable factors of the digital elevation model, slope map, distance from roads, rivers, and buildings, and population density were fed into the model to generate a land cover change map that depicts the changing pattern. In addition, LULC transitions were predicted for 2025 and 2029 based on classified raster images from 2015 and 2017. Future LULC maps were predicted, assuming that the current LULC pattern and dynamics continue.

Before beginning the potential transition modeling with CA-ANN, various operational parameters should be entered into the MOLUSCE plugin. It has six parameters: Random Samples, Neighborhood, Learning Rate, Momentum, Maximum Iterations, and Learning Procedure; these parameters were chosen based on the literature and the importance of the study. During transition modeling, 1000 randomly selected pixels were used for the sample, and ten hidden layers were chosen for the precise prediction of the LULC classes for the year 2021. Furthermore, the momentum of 0.05, the learning rate of 0.1, and neighborhood size (1*1) are the other selected parameters that connect the CA-ANN model's three layers (Input, Hidden, and Output). The resulting prediction was validated to assess the CA-ANN model's ability to predict LULC for the years 2025 and 2029 in the study area. During this step, an actual LULC raster map for 2021 and a simulated LULC raster map for 2021 were inserted into the plugin's 'Validation' tab. This step produced two primary outputs: the percent correctness and kappa (overall). This step was repeated iteratively until the desired accuracy was achieved. Several simulations were run to forecast the LULC change map for 2021 using various combinations of spatial variable factors. The analysis combined two to three spatial variables to create an ANN-Multi layer perception.

2.3. Flood model simulation

The calibrated Las Nieves Floodplain hydrologic model was created using the Hydrologic Engineering Center Hydrologic

Modeling System (HEC HMS) Version 3.5. For this study, we used the Rainfall Intensity Duration Frequency (RIDF) of the Butuan PAGASA Weather Station, which is closest to the basin. The duration of these extreme rainfall events is referred to as the "return period." In HEC HMS, a 24-hour rainfall scenario was created for each rain return period, with the rain peaking at the sixth hour from the start of the simulation. The Las Nieves Floodplain was modeled in 2D, with no 1D elements present. A 2D flow area representing the entire floodplain was created. Las Nieves' 2D flow area mesh has an approximate area of 141.284 km2 and was generated using a 40-m by 40-m cell size. The 2D flow area was finally computed to have 91 855 cells using break lines representing roads, dikes, levees, and riverbanks. A 1-m spatial resolution LiDAR-derived DTM and Manning's roughness coefficients extracted from the various land cover maps were used as inputs to set the model's geometric data.

2.4. Flood Map Generation and Impact Assessment of Various Land Covers

The calibrated HEC HMS model's flow hydrographs were used as inputs into the HEC RAS 2D hydraulic model to predict or estimate flood depths and extents. 2D Boundary Condition for Las Nieves Floodplain hydrograph depicts the flow of water into the domain of the 2D model corresponding to the boundary conditions set. The unsteady flow analysis module of HEC RAS used these flow hydrographs and time series of rainfall to dynamically simulate the depth and extent of flooding. A spatially distributed grid of maximum flood depths was generated for each extreme rainfall event flood simulation. In the GIS software ArcGIS, the depth grid was then exported as a raster file to intersect with the different land cover maps in flooded generating areas to assess each class's impact. Flooding impacts were evaluated by spatially overlaying land cover maps with flood depth maps generated by ArcGIS software for various rainfall events. The flooding impact on land cover classes was determined by computing the inundated areas for each class for all occasions.

3. RESULTS AND DISCUSSION

3.1. Base land cover map

Using Sentinel-2 images with a 10-meter resolution and supervised (SVM) classifier, the land cover map of Las Nieves’ floodplain is generated, shown in Figure 2. The eight classes are Annual Cropland (sage dust), Built-up (mars red), Open Forest (leaf green), Shrubs (light apple), Barren (cocoa brown), Grassland (lemongrass), Perennial Cropland (dark olivenite), and Water (big sky blue). Its total land area is 141.25 sq. km. Among the eight classes situated in the said floodplain, the land class that has the largest coverage is Perennial Cropland with 51.76% (73.11 sq. km), followed by Annual Cropland and Shrubs with 24.38% (34.43 sq. km) and 15.65% (22.10 sq. km), respectively.

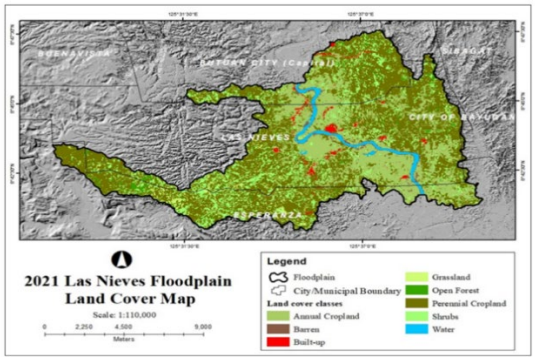

Figure 3. The 2021 Las Nieves floodplain land cover map.

3.2. Base land cover map

Based on the accuracy assessment of the base year 2021 image, the land cover classification results for the whole Las Nieves municipality had an overall accuracy of 94.07% and a kappa of 0.93.

3.3. Predicted land cover maps

Given the 2015 and 2017 land cover maps, the first prediction output was for 2019. For the second iteration, it gave out the 2021 land cover prediction that was also subjected to the validation tab included in the MOLUSCE plugin. The spatial variable combination of the digital elevation model (DEM), distance to roads and buildings, and population density generated a high kappa overall of 0.75, which was considered acceptable for most research. A confusion matrix was made to supplement the output kappa overall obtained using the validation tab in the MOLUSCE plugin. Using the said plugin in QGIS, the following maps were the predicted land cover maps for 2025 and 2029, shown in Figures 4 and 5.

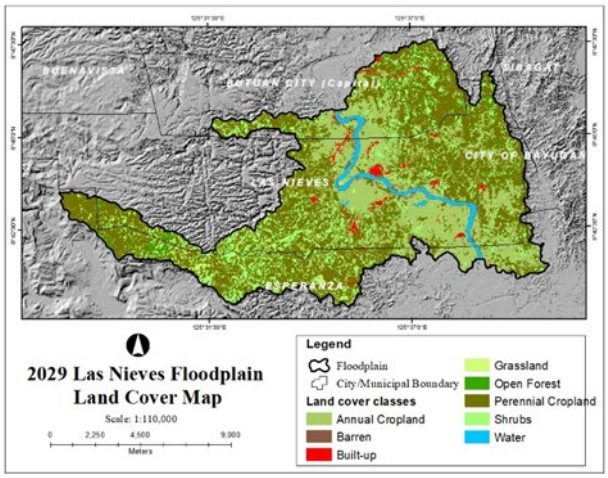

Figure 4. Predicted 2025 land cover map

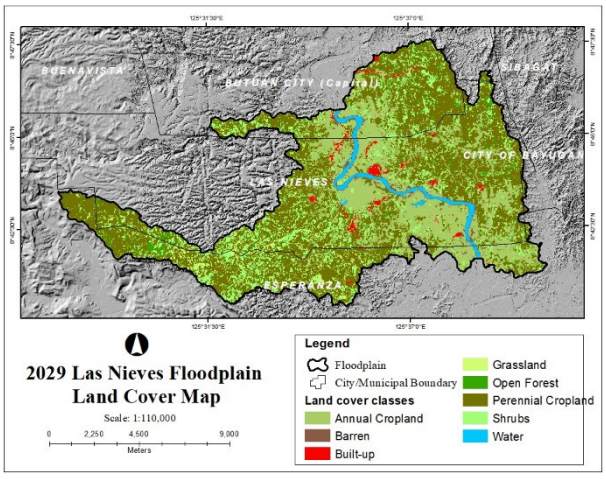

Figure 5. Predicted 2029 land cover map

3.4. Change detection and scenario-based increase built-up

There were minimal spatial changes to the land cover categories from 2025 – 2029. As computed, the % change of annual cropland is only -0.03%. The negative value indicates a decrease from 2015 to 2029. The other land cover with detected change is the built-up with a change of +0.03, indicating an increase from

2025 to 2029. No changes were detected in other land cover classes. Since the predicted land cover models only depicted a small amount of land cover changes, the researchers then edited another projected map layout shown in Figure 6 based on the 2017-2025 Comprehensive Land Use Plan (CLUP) provided by the Local Government Unit (LGU) of Las Nieves. The small changes could be attributed to the spatial variable inputs used as the prediction using MOLUSCE was dependent on, and the land cover periods (e.g., 4-year interval) considered in this study. For the scenario-based class editing, changes of the land cover classes were aligned from the approved CLUP. The increase in Built-up class was near the available expansion of approximately 1,496.85 hectares comprising 10% of the A/D Lands of the Municipality with a total of 1,237.85 hectares.

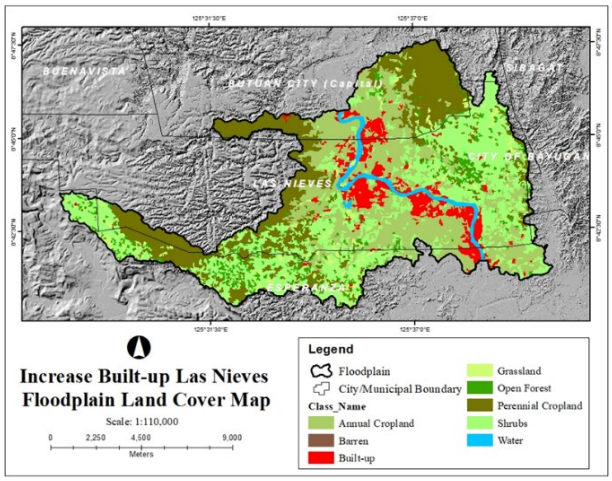

Figure 6. Increase built-up scenario of Las Nieves floodplain.

3.5. Flood depth maps and impact assessment

The generated flood depth maps of Las Nieves floodplain for the 6 extreme rainfall events were generated shown in Figures 7 to 12. It was found that as the rainfall return period increased, the extent of flooding on different land cover also increased. The area of inundated land cover was discovered to increase as the rainfall event return period increased.

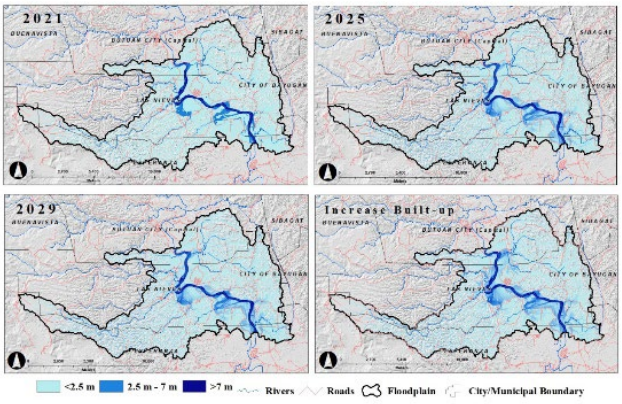

Figure 7. Flood depth maps with a 2-year rainfall return period

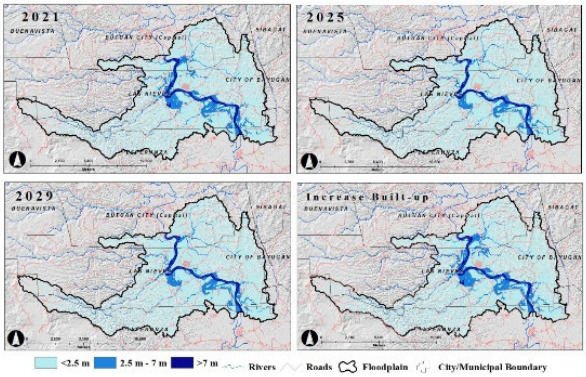

Figure 8. Flood depth maps with a 5-year rainfall return period

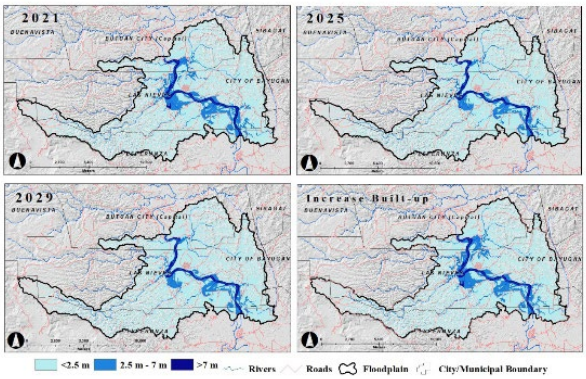

Figure 9. Flood depth maps with a 10-year rainfall return period

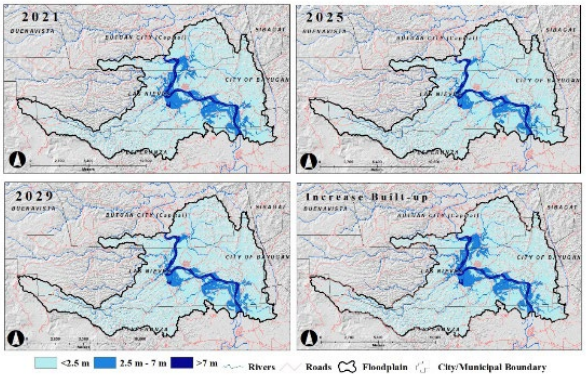

Figure 10. Flood depth maps with a 10-year rainfall return period

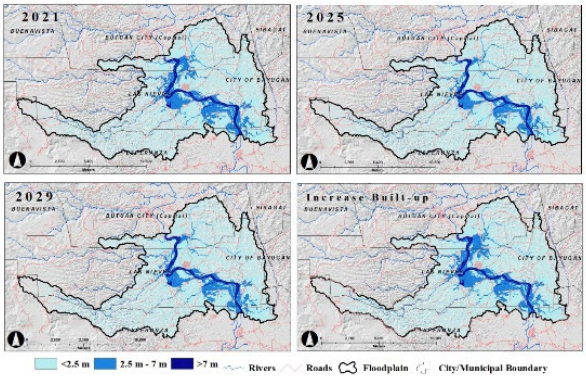

Figure 11. Flood depth maps with a 50-year rainfall return period

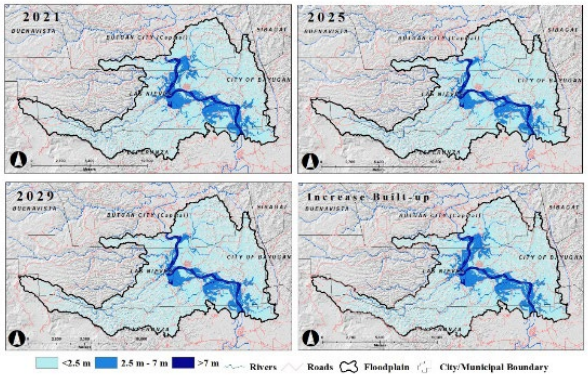

Figure 12. Flood depth maps with a 100-year rainfall return period

The succeeding graphs depict the results of assessing the effects of flooding on various land cover types in the Las Nieves Floodplain area. The area of inundated land cover was discovered to increase as the rainfall event return period increased.

For the 2-year return period as shown Figure 13, among all the land cover classes, annual cropland areas are among the most affected for the year 2021, 2025, 2029, and Increase Built-up with 50.74%, 48.02%, 47.96%, and 39.31% inundated, respectively, followed by perennial cropland with 25.17%, 25.97%, 25.95% inundated for years 2021, 2025, and 2029 respectively, while for the Increase Built-up, built-up comes next with 23.40% inundated. The least affected class for 2021 is open forest with 0.62% inundated, for 2025 is built-up with 0.67% inundated, for 2029 is open forest with 0.68% inundated, and barren with 0.57% inundated for the Increase Built-up.

For the 5-year return period as shown Figure 14, the most affected class is annual cropland for the four land covers with 53.19%, 51.43%, 51.37%, and 46.42% inundated for 2021, 2025, 2029, and Increase Built-up, respectively. It is followed by perennial cropland with 24.91%, 25.00%, and 24.98% inundated for 2021, 2025, and 2029, respectively while built-up with 20.79% inundated for Increase Built-up. The least affected class for 2021, 2025, and 2029 is open forest with 0.57%, 0.62%, and 0.62% inundated, while for Increase Built-up is barren with 0.47%.

For the 10-year return period as shown Figure 15, annual cropland is the most affected class for 2021, 2025, 2029, and Increase Built-up with 54.18%, 52.32%, 52.24% and 48.62 % inundated, respectively. It is followed by perennial cropland with 24.66%, 25.05%, and 25.04% inundated for 2021, 2025, and 2029, respectively while built-up with 19.95% inundated for Increase Built-up. The lease affected class for 2021, 2025, and 2029 is open forest with 0.55%, 0.60%, and 0.60% inundated, respectively and barren with 0.47% for Increase Built-up.

For the 25-year return period as shown Figure 16, the most affected land cover class is annual cropland for 2021, 2025, 2029, and Increase Built-up with 54.63%, 53.24%, 53.13%, and 50.46% inundated respectively. It is followed by perennial cropland with 24.62%, 25.03%, and 24.99% inundated for 2021, 2025, and 2029, respectively while built-up with 19.29% inundated for Increase Built-up. The least affected class for 2021, 2025, and 2029 is open forest with 0.56%, 0.59%, and 0.59% inundated, respective, and barren with 0.44% for Increase Built-up.

For the 50-year return period as shown Figure 17, annual cropland has the most area affected with 54.67%, 53.96%, 53.90%, and 51.09% inundated for 2021, 2025, 2029, and Increase Built-up. It is followed by perennial cropland with 24.71%, 24.76%, and 24.74% inundated for 2021, 2025, and 2029, respectively while built-up with 18.99% inundated for Increase Built-up. The least class affected for 2021, 2025, and 2029 is open forest with 0.57%, 0.58%, and 0.58% inundated, respectively, while barren with 0.42% inundated for Increase Built-up.

For 100-year return period as shown in Figure 18, annual cropland is still the most affected land cover class for 2021, 2025, 2029, and Increase Built-up with 54.63%, 54.43%, 54.33%, and 51.55% inundated, respectively. It is followed by perennial cropland with 24.78%, 24.61%, and 24.56% inundated for 2021, 2025, and 2029, respectively while built-up with 18.75% inundated for Increase Built-up. The least affected class for 2021, 2025, and 2029 is open forest with 0.57%, 0.59%, and 0.59% inundated, respectively while for Increase Built-up is barren with 0.41% inundated.

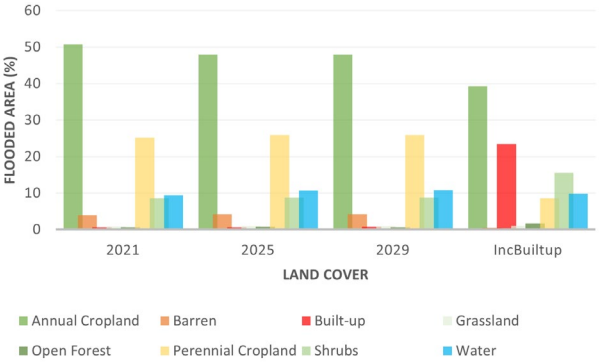

Figure 13. Flooded areas for each land cover with a 2-year rainfall return period.

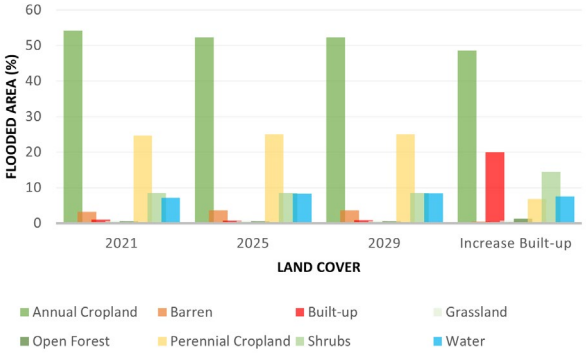

Figure 14. Flooded areas for each land cover with a 5-year rainfall return period.

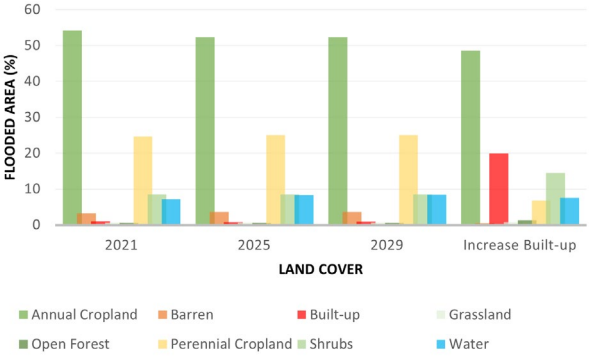

Figure 15. Flooded areas for each land cover with a 10-year rainfall return period.

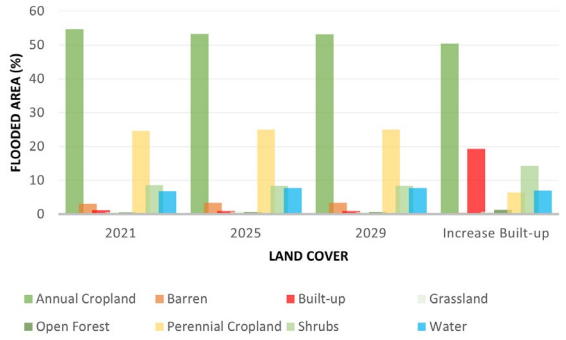

Figure 16. Flooded areas for each land cover with a 25-year rainfall return period.

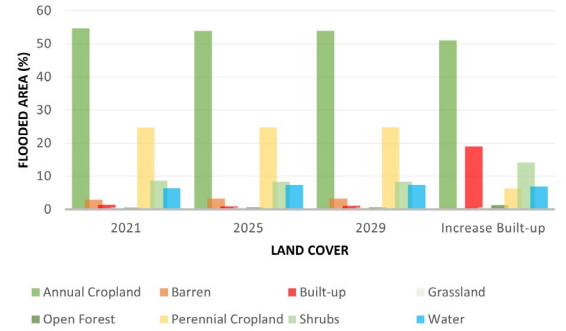

Figure 17. Flooded areas for each land cover with a 50-year rainfall return period.

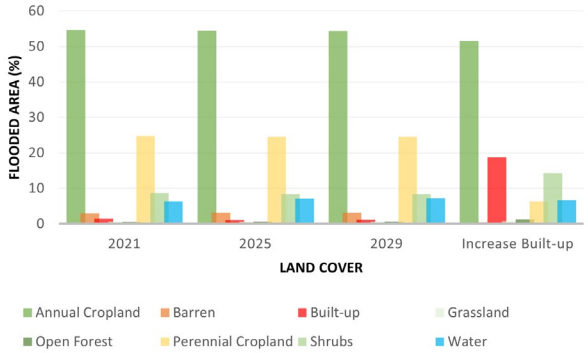

Figure 18. Flooded areas for each land cover with a 100-year rainfall return period.

4. CONCLUSION AND RECOMMENDATIONS

The prediction of land cover maps was used to present a detailed assessment of flooding. This approach was found to be very useful in assessing the flooding impacts of extreme rainfall events on the different land cover years within the Las Nieves floodplain. The generated prediction of future land cover maps was analyzed to extract projected land cover changes of the study area and how these changes affected flooding scenarios during extreme rainfall events. It was shown in the prediction that the future trend of the land cover of the Las Nieves floodplain had a relatively low transition rate concerning the existing spatial driving factors.

Detailed information on potentially affected land cover classes was determined using a high spatial resolution digital terrain model, Sentinel-2 satellite image, prediction of future land cover using spatial variable factors, and flood models. The assessments' findings indicated an increase in areas of inundated land cover as rainfall events became more extreme. The Annual Cropland was the most affected land cover class among the various land cover maps. It was followed by Perennial Cropland, while the least affected land cover class for years 2021, 2025, and 2029 was Open Forest. However, the scenario-based Increase Built-up land cover map was the least affected Barren. In the Increased Built-up scenario, when there was a significant increase in the built-up class, its inundated area also increased. It was worth noting that the areas of the most affected types were near the river. MOLUSCE plugin has successfully predicted future land cover maps and utilized them for flood impact assessment. Notably, the plugin is inherently dependent on the spatial variable factors as inputs to predict future land covers.

5. ACKNOWLEDGEMENT

The Caraga Center for Geo-informatics (CCGeo) provided the flood models used in this study. In addition, ancillary information such as the comprehensive land use plan of the Municipality of Las Nieves, Agusan del Norte, were obtained to supplement the data needed for this research work. We acknowledge the ENGAGE Caraga Project 3 that assisted us in the land cover mapping and prediction and the flood model simulation. We also acknowledge the support extended by the Local Government of Las Nieves during the conduct of the study.

6. REFERENCES

Alam, N., Saha, S., Gupta, S., & Chakraborty, S. (2021). Prediction modelling of riverine landscape dynamics in the context of sustainable management of floodplain: a Geospatial approach. *Annals of GIS*, *27*(3), 299–314. https://doi.org/10.1080/19475683.2020.1870558

Brevante, B. M. (2017). *Analyzing the Effects of Land Cover / Land Use Changes on Flashflood: A Case Study of Marikina River Basin (MRB), Philippines (M. Sc. Thesis)*. 62. https://webapps.itc.utwente.nl/librarywww/papers_2017/msc/aes/brebante.pdf

de Moel, H., & Aerts, J. C. J. H. (2011). Effect of uncertainty in land use, damage models and inundation depth on flood damage estimates. *Natural Hazards*, *58*(1), 407–425. https://doi.org/10.1007/s11069-010-9675-6

Džubáková, K. (2010). Rainfall-Runoff Modelling: Its Development, Classification and Possible Applications. *Acta Geographica Universitatis Comenianae*, *54*(2), 173–181.

Hassan, Z., Shabbir, R., Ahmad, S. S., Malik, A. H., Aziz, N., Butt, A., & Erum, S. (2016). Dynamics of land use and land cover change (LULCC) using geospatial techniques: a case study of Islamabad Pakistan. *SpringerPlus*, *5*(1). https://doi.org/10.1186/s40064-016-2414-z

Reynard, N. S., Prudhomme, C., & Crooks, S. M. (2001). Potential Effects of Changing Climate and Land Use. *Climatic Change*, *48*, 343–359.

Santillan, J. R., Amora, A. M., Makinano-Santillan, M., Marqueso, J. T., Cutamora, L. C., Serviano, J. L., & Makinano, R. M. (2016). Assessing the impacts of flooding caused by extreme rainfall events througha combined geospatial and numerical modeling approach. *International Archives of the Photogrammetry, Remote Sensing and Spatial Information Sciences - ISPRS Archives*, *41*, 1271–1278. https://doi.org/10.5194/isprsarchives-XLI-B8-1271-2016